RSC Advances

ROYAL SOCIETY OF CHEMISTRY

www.rsc.org/advances

Largely enhanced porosity of stretched polypropylene/graphene oxide composite membrane achieved by adding pore-forming agent

Jian Dai[1], Xian-ling Xu[1], Jing-hui Yang[1], Nan Zhang[1], Ting Huang[1], Yong Wang[1*],

Zuo-wan Zhou[1], Chao-liang Zhang[2]

1. Key Laboratory of Advanced Technologies of Materials (Ministry of Education), School of

    Materials Science & Engineering, Southwest Jiaotong University, Chengdu, 610031, China

2. State Key Laboratory of Oral Diseases, Sichuan University, Chengdu, 610041, China

Abstract: A few amount of graphene oxide (GO) was incorporated into polypropylene (PP) to prepare the composite membrane assisted with pore-forming agent polyoxyethyleneoctylphenyl-10 (OP-10). The composite membrane was obtained through melt-compounding and subsequent tensile process. The dispersion of GO in the composite, the dynamic mechanical properties as well as the melting and crystallization behaviors of melt-compounded samples were investigated to clearly understand the initial microstructures of samples. Different tensile strains were applied to obtain the stretched PP composite membrane, and then the morphologies of the composite membrane and the porosity were comparatively investigated. The results showed that the dispersion of GO was apparently improved with the aid of OP-10 and many initial pores were simultaneously introduced into PP/GO/OP-10 composite, which induced the slight decrease of storage modulus and glass transition temperature of PP matrix. OP-10 suppressed the crystallization of PP matrix while GO compensated this effect. Either for the stretched PP/OP-10 or for the composite membranes, they exhibited larger mean pore size compared with the stretched pure PP membrane. Furthermore, compared with the stretched PP, PP/GO and PP/OP-10 membranes, largely increased porosity was achieved for the stretched PP/GO/OP-10 composite membrane, especially at relatively high tensile strain. In addition, it was suggested that the initial pores, which were introduced by adding OP-10, acted as the stress concentrator, promoting more pores formation during the tensile process through inducing the lamellar separation and breakage. This work provided a new method for the preparation of PP-based composite membrane and also endowed it with great potential in many fields.

---

[*] Corresponding author: Tel: +86 28 87602714;
E-mail: yongwang1976@163.com

1

1. Introduction

PP is regarded as an ideal row material for the preparation of membrane due to its good processability, good mechanical properties, excellent chemical stability and thermal stability. To date, PP has been widely applied into the porous membrane preparation mainly through thermally-induced phase separation [1,2] and stretching method.[3-6] In terms of thermally-induced phase separation, PP and other components are firstly dissolved into a certain solvent to form the homogenous solution at high temperature, and the phase separation happens as the temperature decreases. Once the residual solvent is removed, the porous membrane is obtained.[1,2] For stretching method, the melting PP-based composite is treated to obtain the precursor membrane with oriented structure, and then the precursor membrane is stretched at low or high temperature to induce the formation of pores through the breakage or separation of lamella.[7,8] With advantages of simple preparation process, low cost, avoidance of solvent contamination and recovery and so on, the stretching method has attracted much more attention recently. The pore formation behavior of PP membrane is greatly influenced by many factors including material parameters [3,9] and processing parameters.[10-13]

As a new kind of functional nanofiller, graphene oxide (GO) exhibits good reinforcement effect due to its excellent mechanical properties, and therefore, it has been widely used to prepare the reinforced composites.[14] GO also exhibits the good absorbability, which endows it with great potential application in waste water treatment.[15-18] To date, introducing GO into membrane has attracted much attention of researchers, and many GO-based composite membranes have been developed, including poly(vinylidene fluoride) /GO membrane,[19-21] polyethersulfone/GO,[22] chitosan/graphene oxide.[23] However, rare work has been carried out to prepare PP/GO composite membrane. Ramasundaram S. *et al.*[24] prepared PP fiber/reduced graphene oxide (rGO) composite membrane. RGO with high coating density was well dispersed in matrix through a three-step dip-coating method. The results showed that the highly hydrophobic surface was obtained and the excellent performance in terms of the water flux and trans-filter pressure was further demonstrated for rGO-coated PP fiber membrane. But it should be noted that the high hydrophobicity might lead

to the contamination of membrane surface on one hand. On the other hand, the complex preparation steps could not be suitable for membrane preparation. In our previous work,[25] we attempted to prepare β-nucleated PP/GO composite membrane through stretching method. The results showed that the presence of GO resulted in the formation of pores with relatively smaller mean pore size in all conditions, especially at relatively high stretching temperature and/or tensile speed, and it induced porosity enhancement in the stretched sample. However, it should be stressed that the porosity was not high enough in spite of the presence of amounts of β-phase with loose lamellae arrangement that usually facilitated the pore formation of stretched membrane.[10,26] Therefore, more work needs to be done to further enhance the porosity of the PP/GO composite membrane.

To obtain PP membranes with well-controlled structure and excellent comprehensive properties, lots of attempts have been made through compounding or blending with other components.[27-32] For example, Goodarzi V *et al.*[27] prepared PP/ethylene vinyl acetate copolymer (EVA)/clay composite membrane with the aid of a compatibilizer. Different morphologies were obtained through adjusting the content of the component and/or fillers, which resulted in the change of selective gas permeability behavior. Tabatabaei SH *et al.*[28] prepared the blend membrane using two linear PP with different molecule weights through stretching method. Bigger pore density and more uniform pore size were obtained as the amount of high molecular weight component increased. Meanwhile, the interconnectivity of pores was also increased, which leaded to the improvement of permeability. What's more, PP/diluent composite membrane was also widely prepared through thermal phase separation method. Dibutyl phthalate (DBP),[33] diamyl phthalate (DAP) [34] or some other compounds were used as the diluent in order to introduce pores during the phase separation process,[35,36] and the pore formation behavior could be well controlled through adjusting the diluent content and thermal phase separation conditions.

Pore-forming agent, as an effective additive for facilitating the pore formation of materials, is widely applied during the preparation and/or modification of porous membrane.[37-39] With the assistance of the pore-forming agent, the structure of the matrix becomes loose, which is in favor of the pore formation during the stretching process. And also, the stress field in the sample can be changed with introducing the initial pores, which may trigger the formation of new pores around the initial pores during the stretching process.

3

In this work, we attempt to introduce pore-forming agent, i.e. polyoxyethyleneoctylphenyl-10 (OP-10), into PP/GO composite membrane. OP-10 is a kind of amphiphilic pore-forming agent with methyl on one side and hydroxyl on the other. The pore formation mechanism is possibly related to the following two aspects.[40] First, during the melt-compounding process, OP-10 has a tendency to distribute at the interface between the melt of PP and air when the droplets of PP are melted. In this condition, the migration of air becomes more difficult and it forms the bubbles in the PP melt. Second, OP-10 also improves the stabilization of the bubbles. The effects of GO and OP-10 on the pore formation behaviors of PP, including the pore morphology and porosity obtained at different tensile strains, are investigated in details. Interestingly, with the assistance of OP-10, largely enhanced porosity is achieved for the stretched PP/GO/OP-10 composite membrane. This endows the PP/GO/OP-10 composite membrane with great potential application in many fields.

2. Experimental part

2.1 Materials

PP (trade name of PP140) with melt flow rate (MFR) of 4.6 g/10min (190 °C/2.16kg) was obtained from Kaikai Petrochemical Corporation, China. Graphite was obtained from Qingdao Heilong Graphite Co., Ltd. The pore-foaming agent OP-10 was supplied by Chengdu Kelong Chemical Reagent Factory, China. The chemical structural formula of OP-10 is:

$$C_8H_{17}-\!\!\!\!\bigcirc\!\!\!\!-(OCH_2CH_2)_{10}OH$$
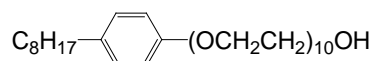
2.2 Sample preparation

GO was prepared in our lab according to the modified Hummer's method.[41] After that, some functional groups, including carboxyl and hydroxyl groups, were introduced to the surface of the GO. The corresponding data relating to the microstructure of the GO can be seen in our previous work.[42]

In this work, four different samples, i.e. neat PP, PP/GO containing 0.5 wt% GO, PP/OP-10 containing 5 wt% OP-10, and PP/GO/OP-10 containing 5 wt% OP-10 and 0.5 wt% GO were simultaneously prepared through the melt compounding processing, which was conducted on a twin-screw extruder SHJ-20 (Nanjing Ruiya, China) at a screw speed of 200 rpm and the melt temperatures of 150-160-175-190-200-200-195 °C from hopper to die. In terms of PP/GO-OP-10

sample, it is worth noting that before melt compounding of the sample, OP-10 and GO were first dissolved in the Dimethl Formaide (DMF) to improve the dispersion of GO. Then, the GO/OP-10 solution was poured into PP powder and the mixture was dried at 80 °C until DMF was completely removed. After being granulated, the pellets of material were compression-molded at the melt temperature of 200 °C and the pressure of 5 MPa to obtain the dumbbell sample with a length of 112 mm, a width of 10 mm and a thickness of 0.1 mm.

2.3 Optical microscopy (OM)

A transmission optical microscope (TOM) AXIO Imager A1m (ZERSS, Germany) was used to characterize the dispersion of GO in the samples. The sample slice was compression-molded using the extrudate and the thickness of the sample slice was about 20 μm.

2.4 Transmission electron microscopy (TEM)

The dispersion of GO and the presence of initial pores in the composite were further investigated using a transmission electron microscopy (TEM) JEM-2100F (JEOL, Japan) with operating voltage of 200 kV. An ultrathin section with a thickness of about 90 nm, which was cut using a cryo-diamond knife on a microtome EM UC6/FC6 (LEICA, Germany), was used for TEM characterization.

2.5 Dynamic mechanical analysis (DMA)

The dynamic mechanical properties were measured using a dynamic mechanical analysis (DMA) Q800 (TA Instruments, USA). The tensile mode was selected. A rectangular sample, which was directly cut from the compression-molded bar, was used and it had a length of 33 mm, a width of 10 mm and a thickness of about 0.1 mm. The measurement was carried out from -50 to 150 °C at a heating rate of 3 °C/min and a frequency of 1 Hz.

2.6 Differential scanning calorimetry (DSC)

A differential scanning calorimetry (DSC) STA449C Jupiter (Netzsch, Germany) was used to investigate the crystalline structure of the sample. For the sample without tensile measurement, it was heated from 30 to 200 °C at a heating rate of 10 °C/min and maintained at 200 °C for 5 min to erase thermal history, then the sample was cooled down to 30 °C at a cooling rate of 5 °C/min. For the stretched sample, it was directly heated from 30 to 200 °C at the heating rate of 10 °C/min. For each measurement, the weight of sample was maintained at 8 mg and the measurements were

carried out in the nitrogen atmosphere. The degree of crystallinity (X_{c-DSC}) can be calculated according to the following relation:

$$X_{c-DSC} = \frac{\Delta H_m}{\phi \cdot \Delta H_m^0} \times 100\% \qquad (1)$$

Where ΔH_m is the DSC measured value of fusion enthalpy obtained during the heating process, ΔH_m^0 is the fusion enthalpy of the completely crystalline polymer, and ϕ is the weight fraction of PP in the sample. Here, the ΔH_m^0 of PP was selected as 177 J/g.[43]

2.7 Wide angle X-ray diffraction

The crystalline structures of PP matrix in different samples were investigated using a wide angle X-ray diffraction (WAXD, Panalytical X'pert PRO diffractometer with Ni-filtered Cu Kα radiation, the Netherlands). The continuous scanning angle range was set from 5° to 35° and the measurement was carried out at 40 kV and 40 mA. The degree of crystallinity (X_{c-WAXD}) was calculated according to the following relation:

$$X_{c-WAXD} = \frac{\sum A_{crystalline}}{\sum A_{crystalline} + \sum A_{amorphous}} \times 100\% \qquad (2)$$

where $A_{crystalline}$ and $A_{amorphous}$ represent the integrated intensities under the crystalline peaks and the integrated intensities under the amorphous halo. It is worth noting that the intensities for a given scattering angel was integrated azimuthally to reduce the possible effect of orientation.

2.8 Tensile experiment

The tensile experiment was conducted on a high-temperature creeping instrument M-4020 (REGER, China). Different tensile strains (0 %, 50 %, 100 % and 200 %) were selected at the ambient temperature of 100 °C. After stretching, all the samples were maintained at 100 °C for 5 min to stabilize the pore morphology.

2.9 Scanning electron microscopy (SEM)

The pore morphology was characterized using a scanning electron microscope (SEM) Fei Inspect (FEI, the Netherlands) with an accelerating voltage of 20.0 kV. Before SEM characterization, all the samples were sputter-coated with a thin layer of gold. To accurately make a comparison of pore

morphology among different samples, the mean pore size was calculated. It is worth noting that in the present work, the size of the pore was defined as the pore length along the tensile direction. When calculating the mean pore size, at least 200 pores from the different zones of the sample were measured and the data were obtained using the software Nano Measurer 1.2.

2.10 Porosity measurement

The porosity (A_k) of the stretched membrane was measured through the following procedures: the stretched membrane was immersed in ethanol for 24 h, after that, the membrane was taken out and the ethanol on the membrane surface was carefully removed using filter paper. Finally, the treated membrane was weighted carefully. The porosity was calculated according to the following relation: [44]

$$A_K = \frac{(w_0 - w)\overline{\rho}}{\overline{\rho}w_0 - (\rho - \overline{\rho})w} \times 100\% \qquad (3)$$

where w is the initial membrane weight, w_0 is the immersed membrane weight. ρ (0.8 g/cm^3) and $\overline{\rho}$ (0.91 g/cm^3) are the density of ethanol and PP, respectively.

3.   Results and discussion

3.1 Microstructure of sample as prepared

The dispersion of GO in the PP/GO and PP/GO/OP-10 composites were firstly characterized using TOM. As shown in Figure 1, GO exhibits relatively poor dispersion in the PP/GO composite. However, with the presence of OP-10, the dispersion of GO is apparently improved and the size of GO agglomerates is greatly decreased. To further understand the dispersion state of GO and the morphology of initial pores in the sample, the representative PP/GO/OP-10 composite was further characterized using TEM. As shown in Figure 2, at relatively low magnification, there are many initial pores in the sample, indicating that OP-10 is an effective pore-forming agent and it successfully induces the formation of initial pores. Furthermore, one can see that the dispersion of initial pores is not homogeneous. Besides the presence of large pores with diameter up to 500 nm, some very small pores with diameter of about 60 nm can be also seen. The sheet-like structure of GO can be differentiated at relatively high magnification. It is worth noting that GO is mainly dispersed around the initial pores. This is possibly related to the good interfacial interaction

between OP-10 and GO. As shown previously, OP-10 is the amphiphilic pore-forming agent with methyl on one side and hydroxyl on the other. GO is also an amphiphilic filler with many functional groups on the edge of the sheet, including carboxyl and hydroxyl groups.[45] Specifically, the sample preparation method that is carried out in the present work also provides more probability for the interaction between OP-10 and GO.

Figure 3 exhibits the dynamic mechanical properties of all samples. From Fig. 3a one can see that pure PP exhibits glass transition temperature (T_g) of 12.8 °C. Slightly decreased T_g (12.0 °C) is observed for the PP/GO sample possibly due to the slightly increased free volume induced by the presence of GO. More apparent decrease of T_g is observed for the PP/OP-10 sample, and it shows T_g of 10.3 °C. This indicates that the chain segment mobility is enhanced due to the presence of OP-10. In other words, OP-10 can be thought as a plasticizer of PP possibly due to the presence of many pores that increase the free volume of material, which is favorable for the motion of PP chain segments. The T_g of the PP/GO/OP-10 sample is slightly higher than that of PP/OP-10 sample but still smaller than those of pure PP and PP/GO samples. This is possibly related to the improved dispersion of GO particles that decrease the chain segment mobility of PP matrix to a certain extent. It should be stressed that the measurement was repeated for several times and the similar variation trend was observed. Therefore, the data have a statistical significance. From Fig. 3b one can see that the presence of GO induces the slight decrease of storage modulus (E') of the PP/GO sample, but more apparent decrease of E' is observed for the PP/OP-10 sample, especially at temperatures below glass transition temperature (T_g) of PP matrix. This further indicates the plasticizing effect of OP-10. In the whole measuring temperature range applied in this work, the PP/GO/OP-10 composite exhibits the similar E' to that of the PP/OP-10 sample. Generally, well-dispersed GO can exhibit good reinforcement effect for polymer.[46] However, in this work, either for the PP/GO sample or for the PP/GO/OP-10 sample, the E' is lower than that of the pure PP. This is possibly related to the relatively poor dispersion of GO in the PP/GO sample and the apparent plasticizing effect of OP-10 in the PP/GO/OP-10 sample, respectively.

The melting and crystallization behaviors of different samples were investigated using DSC, and the results are shown in Figure 4. From Fig. 4a one can see that pure PP exhibits a strong

endothermic peak at 166.0 °C and a very weak peak at about 146.1 °C, attributing to the fusion of

α-form PP ($T_{m\alpha}$) and β-form PP ($T_{m\beta}$), respectively. In terms of the PP/GO sample, double

endothermic peaks are present at about 159.3 and 165.8 °C. This is consistent with the results

reported in the literatures that GO is an α-form nucleating agent of PP.[47] For the PP/OP-10 sample,

the intensity of the endothermic peak of β-form PP is increased, which indicates the increased

amount of β-form PP in the sample. Furthermore, the endothermic peak of α-form shifts to lower

temperature (161.4 °C), indicating that the lamellar thickness of α-form PP in the PP/OP-10 sample

is smaller than that in the pure PP. Interestingly, compared with the PP/OP-10 sample,

PP/GO/OP-10 sample exhibits weaker endothermic peak of β-form PP on one hand. On the other

hand, double endothermic peaks are present again at 161.1 and 165.0 °C. This further indicates that

GO is the α-nucleating agent of PP and it suppresses the nucleation and growth of β-form PP in the

PP/GO/OP-10 sample. In other words, there is a competition between OP-10 and GO in inducing

crystallization of PP matrix. The crystallinity (X_{c-DSC}) was calculated and the results are also

shown in Fig. 4a. One can see that pure PP exhibits the biggest X_{c-DSC} while the other three

samples exhibit relatively lower X_{c-DSC}. This is also one of the reasons why the other three

samples exhibit smaller storage modulus compared with pure PP as indicated in Fig. 3b.

As shown in Fig. 4b, compared with the crystallization of pure PP that exhibits the crystallization

temperature (T_c) of 119.8 °C, the PP/GO sample exhibits higher T_c (122.6 °C), further indicating

the nucleation effect of GO on PP crystallization. However, for the PP/OP-10 sample, it exhibits

lower T_c (117.6 °C). This implies that OP-10 suppresses the crystallization of PP matrix. Because

the crystallization of PP in the PP/OP-10 sample occurs at relatively low temperature, the lamellar

growth becomes more difficult. This is also the reason why the PP/OP-10 sample exhibits lower

$T_{m\alpha}$ compared with pure PP. Due to the nucleating effect of GO, the PP/GO/OP-10 sample exhibits

slightly enhanced T_c (120.6 °C).

To further understand the crystalline structure of PP matrix in different samples, WAXD

measurement was carried out. Figure 5 exhibits the WAXD profiles of different samples. It can be

seen that pure PP exhibits several characteristic diffraction peaks at 2θ=14.3°, 17.0°, 18.7°, 21.2°

and 22.0°, attributing to the reflections of (110), (040), (130), (111) and (131) crystal planes of α-form PP. In addition, a weak diffraction peak at 2θ=14.3°, which is attributed to the reflection of (300) crystal plane of β-form PP, is also observed, indicating the presence of a few amount of β-form PP in the pure PP. The PP/GO sample also exhibits the characteristic diffraction peaks of α-form. Compared with pure PP, the PP/OP-10 sample exhibits stronger diffraction peak of (300) crystal plane, indicating the increased amount of β-form PP in the sample. This agrees well with the observation obtained from DSC measurement as shown in Fig. 4a. The crystallinity of sample was also calculated. As shown in Fig. 5, the four samples exhibit the similar crystallinity. This is slightly different from the observations obtained through DSC measurement. The different variation trends of crystallinity between DSC measurement and WAXD measurement are possibly related to the different characterization methods.

3.2 Effect of OP-10 and GO on pore formation

The pore morphologies of different samples obtained through uniaxial tensile process were characterized using SEM. In this section, the tensile speed was set at 50 mm/min, the ambient temperature was maintained at 100 °C, and the tensile strain was maintained at 100%. The representative SEM images are shown in Figure 6 and the values of mean pore size are also labeled in the images. It can be clearly seen that many pores are successfully created in the stretched membranes. Pure PP membrane exhibits the smallest mean pore size of 193.8 nm while PP/GO and PP/OP-10 membranes exhibit bigger mean pore size of 223.3 and 260.5 nm, respectively. For the PP/GO/OP-10 composite membrane, the mean pore size is about 210.5 nm, which is slightly higher than that of pure PP membrane but apparently smaller than that of PP/OP-10 membrane. It is well known to all that the pore formation during the uniaxial stretching processing is mainly attributed to the lamellae separation along the tensile direction, which is also accompanied by deformation, rotation or breakage of little amount of lamellae arranging along other directions.[48] Furthermore, the molecular chain mobility also influences the nucleation and growth of the pores. Generally, during the tensile process, the enhanced mobility promotes the motion of molecular chains in the interlamellar amorphous and the slippage and separation of the lamellar structure along the tensile direction, and then promotes the nucleation and growth of the pores. Therefore, the largely increased mean pore size in the stretched PP/OP-10 membrane is mainly attributed to the enhanced

chain mobility of PP matrix, which has been shown by the decrease of T_g as shown in Fig. 3. Furthermore, the presence of β-form PP that exhibits the parallel lamellar stacking structure and the α-form with more defects and/or smaller lamellar thickness are possibly the other reasons for the largely increased mean pore size. It has been demonstrated that pores are easily created through the slippage and separation of the parallel lamellar structure when the β-form PP is stretched.[26,48-50] For the PP/GO composite membrane, it exhibits larger mean pore size than that of pure PP. This is possibly related to the presence of relatively larger GO agglomerates, which result in the local stress concentration in the sample, facilitating the nucleation and growth of pores around GO agglomerates through interfacial debonding between PP matrix and GO agglomerates. For the PP/GO/OP-10 composite membrane, the presence of GO possibly restricts the motion of PP chain segments on one hand; on the other hand, GO suppresses the formation of β-form PP and promotes the integration of α-form lamellar structure (seen in Fig. 4). Specifically, the dispersion of GO is apparently improved. In this condition, the growth of pore becomes more difficult. However, the role of OP-10 can not be completely ignored. That is the reason why the mean pore size of the stretched PP/GO/OP-10 composite membrane is smaller than that of the PP/OP-10 membrane but still larger than that of the pure PP membrane.

The evolution of pore morphology during the tensile process of the representative PP/GO/OP-10 composite membrane was then characterized to know the effect of tensile strain on the formation of pores. Figure 7 exhibits the SEM images of the stretched membranes obtained at different tensile strains. The mean pore size of each sample is also shown in the corresponding image. From Fig. 7a one can see that before stretching, sporadic pores are present in the sample, which further demonstrates the pore-forming role of OP-10. After being stretched to a small strain, i.e. 50% (Fig. 7b), the stretched composite membrane exhibits at least two features. First, the initial pores are elongated along the tensile direction. Second, many small pores are introduced into the membrane. The average size of the new pores is about 118.8 nm. With the increase of tensile strain (100%, Fig. 7c), besides the further deformation of the initial pores during the tensile process, much more new pores are introduced on one hand. On the other hand, the mean pore size is increased up to 210.5 nm. This indicates that increasing tensile strain facilitates the increase of pore size and pore number. However, it is worth noting that the increase of mean pore size becomes inconspicuous at relatively

high tensile strain. For example, at tensile strain of 200% (Fig. 7d), the mean pore size is only increased up to 261.2 nm, which is only about 50 nm larger than that of membrane obtained at tensile strain of 100%.

The variation of porosity versus the tensile strain is illustrated in Figure 8. For the stretched PP membrane, there is very small variation in porosity. Specifically, it can be seen that a relatively high tensile strain even induces the slight decrease of porosity. For example, the porosity of stretched PP membrane is decreased from 5% at tensile strain of 100% to 3.1% at tensile strain of 200%. For the stretched PP/GO membrane, the porosity increases gradually with increasing of tensile strain. Although the porosity of the stretched PP/OP-10 membrane also increases gradually with the increase of tensile strain, the porosity is still very low and it is even lower than that of the stretched PP/GO membrane. However, it is interesting to observe that largely enhanced porosity is achieved for the stretched PP/GO/OP-10 membrane at relatively high tensile strain (100 and 200%). For example, at tensile strain of 200%, the porosity is enhanced up to 22.1%. This is even much higher than the porosity of stretched β-form PP membrane obtained in our previous work,[25] in which the porosity was only about 11% when the membrane was prepared under the completely same tensile conditions.

According to the principle of porosity measuring applied in this work, it can be deduced that there are several factors influencing the value of porosity, i.e. the number of pores, the pore size and the polarity of the membrane, etc. Generally speaking, the bigger the number of pore in the stretched membrane is, the larger the porosity is. Although larger pore size facilitates the enhancement of water flux,[51] it is possibly unfavorable for porosity measurement because ethanol can not be stably reserved in the pore with very large size. Increasing polarity of membrane enhances the wettability of membrane, which not only increases water flux but also results in the increase of the measured porosity.[52] As shown in Fig. 6, at the same tensile conditions, stretched PP/OP-10 membrane exhibits the biggest mean pore size while stretched PP membrane exhibits the smallest one. Although the mean pore size of PP/GO/OP-10 membrane is smaller than those of PP/GO and PP/OP-10 membranes, it is worth noting that the polarity of the former sample is higher than that of the latter one. Specifically, at relatively high tensile strain, the presence of many pores as well as the deformation of PP matrix most likely results in more exposed GO particles, which further

increase the polarity of stretched membrane. This can be indirectly demonstrated by the relatively larger porosity of the stretched PP/GO membrane as compared with the stretched PP/OP-10 membrane, although the latter membrane exhibits the larger mean pore size. Furthermore, it can be seen that in the field of view, the number of pores in the stretched PP/GO/OP-10 membrane is much larger than that in the stretched PP/OP-10 membrane. Besides the stress concentrator of initial pores that induces more pores formation around the initial pores through changing the stress field, the debonding of GO particles from PP matrix is possibly the other reason for the increase of pore number. Consequently, largely enhanced porosity is achieved for the stretched PP/GO/OP-10 membrane, especially at relatively high tensile strain.

3.4 Further understanding about the pore formation mechanism

Through introducing pores (or voids) to adjust the mechanical properties of polymer materials has been widely researched elsewhere. For example, Huang Y *et al.*[53] and Bagheri R *et al.*[54] reported that if the void with a micrometer or more in diameter was present, the toughness of the matrix could be significantly enhanced. Specifically, according to the calculation of stress intensity at the early stage of crack growth, they also proposed that the sample containing voids exhibited a greater ability to undergo plastic deformation compared with the sample without voids. In the present work, the tensile process is a quasi-static process, which is apparently different from the dynamic impact process. However, previous results have already shown that with the simultaneous addition of OP-10 and GO, the stretched PP/GO/OP-10 membrane exhibits much higher porosity at relatively high tensile strain (100 and 200%). Therefore, it is expected that the presence of initial pores, which are induced by OP-10, can induce the change of stress field during the tensile process and then induces more pores formation around the initial pores. To demonstrate this, the pore morphology around initial pores was carefully characterized, and the representative images are shown in Figure 9. It is clearly seen that besides the deformation of the initial pores, many small pores are really induced in the adjacent PP matrix around the initial pores. This clearly demonstrates the promotion role of initial pores in inducing new pores formation during the tensile process.

To further understand the pore formation behavior of sample during the tensile process, the crystalline structure evolution of the stretched membrane was then characterized using DSC and WAXD. Figure 10 exhibits the melting behaviors of representative stretched membranes obtained

at a tensile strain of 100%. It can be seen that all the membranes exhibit only one endothermic peak at about 161-164 °C, indicating that only α-form PP is present in the stretched membranes. This means that there is a transition from β-form to α-form during the tensile process.[55] Furthermore, compared with the melting behaviors of samples as shown in Fig. 4a, one can see that except the PP/OP-10 membrane, which exhibits nearly invariant $T_{m\alpha}$ before and after being stretched, the stretched PP, PP/GO and PP/GO/OP-10 membranes exhibit smaller $T_{m\alpha}$ compared with the un-stretched samples. This indicates the occurrence of lamellar separation and/or breakage during the tensile process, which results in the formation of lamellae with more defects and/or thinner lamellar thickness.[56] Figure 11 exhibits the WAXD profiles of the representative stretched PP/GO/OP-10 membranes obtained at different tensile strains. Compared with the WAXD profile shown in Fig. 5, which exhibits the characteristic diffraction peaks of both α- and β-form PP, there are at least two features that need to be noticed. First, all the stretched PP/GO/OP-10 membranes exhibit the diffraction peaks of only α-form PP, further showing the transformation of β-form to α-form PP during the tensile process. Second, it can be seen that the stretched membranes exhibit higher X_{c-WAXD} compared with the initial sample as prepared. For example, the initial sample exhibits the X_{c-WAXD} of 52.9%, while the stretched membranes exhibit X_{c-WAXD} of 61% at tensile strain of 50% and 68.9% at tensile strain of 200%. The increase of crystallinity is most likely ascribed to the second crystallization of PP matrix induced by tensile stress. In addition, the relative size of the largest dimension of crystallite is estimated based on the peak broadening associated with the (110) diffraction peak according to the Scherrer relation:[57,58]

$$D_{(110)} = \frac{\lambda}{B_{(110)} \cos\theta} \qquad (4)$$

where λ is the X-ray wavelength (0.154 nm), $B_{(110)}$ is the (110) diffraction peak width at half the maximum intensity, and θ is half the scattering angle. As shown in Fig. 11b, the crystallite size tends to decrease with increasing of tensile strain. This further implies the destroy of initial crystalline structure through lamellar separation and breakage during the tensile process.

To better understand the pore formation mechanism, more visualized schematic representations are shown in Figure 12. For the PP/OP-10 sample (Fig. 12a), during the uniaxial tensile process, the

initial pores that are introduced by adding OP-10 act as the stress concentrator, which leads to the change of stress field in the adjacent PP matrix. Therefore, the spherulites around initial pores experience intense deformation, leading to more pores nucleation through inducing more lamellar separation and breakage on one hand. On the other hand, because of the plasticizing effect of OP-10, the enhanced chain segment mobility of PP matrix promotes the growth of newly-formed pores in the stress field. Consequently, larger mean pore size is achieved for the stretched PP/OP-10 membrane as shown in Fig. 6. In addition, the presence of a few amount of β-form PP that exhibits parallel lamellar structure is possibly one of the main reasons for the largely increased mean pore size because the parallel lamellar structure has greater ability to be separated compared with the cross-hatched lamellar structure of α-form PP. For the PP/GO/OP-10 sample (Fig. 12b), although the role of OP-10 is still present, the presence of GO particles may prevent the growth of newly-formed pores through restricting the motion of PP chain segments, which results in the formation of pores with smaller size. However, GO also exhibits the stress concentrator, which results in more probability for the lamellar separation and breakage of adjacent PP matrix. Furthermore, the interfacial debonding occurred between GO and PP matrix may increase the number of pores, which facilitates the enhancement of the porosity. With the increase of tensile strain, the interfacial debonding becomes more apparent, resulting more pores formation in the stretched membrane. Consequently, higher porosity is achieved at relatively high tensile strain.

 This work demonstrates that the porosity of stretched PP membrane can be greatly enhanced through simultaneous addition of pore-forming agent and GO, which endows the composite membrane with great potential application in many fields. However, it should be stressed that only one content of OP-10 and/or GO is used in this work. Considering the apparent effect of OP-10 and/or GO on the pore formation behavior of PP membrane, studying on the effect of OP-10 and/or GO content on the pore formation becomes very significant. In addition, although the size of pore was rigorously defined and at least 200 pores were selected during the measurement to insure that the data have a statistical significance, it should be pointed out that the determination of pore size is still relatively rough. Further work needs to be done to adjust the processing parameters so that the stretched PP composite membrane can be accurately characterized through more suited characterization method.

RSC Advances Accepted Manuscript

4. Conclusions

  Four different stretched membranes, including PP membrane, PP/GO composite membrane, PP/OP-10 membrane and PP/GO/OP-10 composite membrane, have been prepared through melt-compounding and subsequent tensile process. The results show that many initial pores can be introduced into PP material through adding OP-10. The presence of OP-10 enhances the chain segment mobility but suppresses the crystallization of PP matrix. There is a competition between OP-10 and GO particles in influencing the crystallization of PP matrix. The presence of initial pores promotes the nucleation and growth of new pores during the tensile process, leading to larger mean pore size for the stretched PP/OP-10 membrane. However, the presence of well-dispersed GO prevents the growth of pore. Largely enhanced porosity is achieved for the stretched PP/GO/OP-10 membrane, especially at relatively high tensile strain. Furthermore, increasing tensile strain facilitates the increase of mean pore size. Further results implies that the initial pores, which are introduced by adding OP-10, act as the stress concentrator, promoting more pores formation during the tensile process through inducing the lamellar separation and breakage.

Acknowledgements

References

[1] H. Matsuyama, H. OIkafuji, T. Maki, M. Teramoto and N. Tsujioka, *J. Appl. Polym. Sci.*, 2002, **84**, 1701

[2] N. Tang , Q. Jia, H.J. Zhang, J. J. Li and S. Cao, *Desalination*, 2010, **256**, 27

[3] S. Farhad, A. Ajji and P. J. Carreau, *J. Membrane Sci.*,2007, **292**, 62

[4] S. H. Tabatabaei, P. J. Carreau and A. Ajji, *J.Membrane Sci.*,2009, **345**, 148

[5] F. Chu and Y. Kimur, *Polymer*,1996, **37**, 573

[6] G. T. Offord, S. R. Armstrong, B. D. Freeman, E. Baer, A. Hiltner ,J. S. Swinnea and D. R. Paul, *Polymer*, 2013, **54**, 2577

[7] M. B. Elias , R. Machado and S. V. Canevarolo, *J. Therm. Anal. Calorim.*, 2000, **59**, 143

[8] K. Y. Lin, M. Xanthos and K. K. Sirkar, *J. Membrane Sci.*,2009, **330**, 267

[9] H. Matsuyama, T. Maki, M. Teramoto and K. Asano, *J. Membrane Sci.*,2002, **204**, 323

[10] G. T. Offord, S. R. Armstrong, B. D. Freeman, E. Baer, A. Hiltner and D. R. Paul, *Polymer*, 2013, **54**, 2796

[11] S. H. Tabatabaei, P. J. Carreau and A. Ajji, *Polymer*, 2009,**50**,4228

[12] C. H. Lei, S. Q.Wu, Q. Cai, R. J. Xu, B. Hu and W. Q. Shi, *Polym. Int.*, 2014, **63**, 584

[13] G. K. Elyashevich, I. S. Kuryndin, V. K. Lavrentyev,A. Yu. Bobrovsky and V. Bukošek, *Polymers*, 2012, **54**, 1907

[14] M. A. Rafiee, J. Rafiee, Z. Wang, H. H. Song, Z. Z. Yu and N. Koratkar, *ACS Nano*, 2009, **3**, 3884

[15] C. A. Crock, A. R. Rogensues, W. Q. Shan and V. V. Tarabara, *Water. Res.*,2013, **47**, 3984

[16] H. M. Sun, L. Y. Cao and L. H. Lu, *Nano. Res.,* 2011, **4**, 550

[17] G. K. Ramesha, A. V. Kumara, H. B. Muralidhara and S. Sampath, *J. Colloid. Interf. Sci.*, 2011, **361**, 270

[18] W. J. Zhang, C. J. Zhou, W. C. Zhou, A. H. Lei, Q. L. Zhang, Q. Wan and B. S. Zou, *Bull. Environ. Contam. Toxicol.*, 2011, **87**, 86

[19] Z. H. Wang, H. R. Yu, J. F. Xia, F. F. Zhang, F. Li, Y. Z. Xia and Y. H. Li, *Desalination*, 2012, **299**, 50

[20] J. G. Zhang, Z. W. Xu, M. J. Shan, B. M. Zhou, Y. L. Li, B. D. Li, J. R. Niu and X. M. Qian, *J. Membrane Sci.*, 2013, **448**, 81

[21] C. Q. Zhao, X. C. Xu, J. Chen and F. L. Yang, *J. Environ. Chem. Eng*., 2013, **1**, 349

[22] S. Zinadini, A. A. Zinatizadeh, M. Rahimi, V. Vatanpour and H. Zangeneh, *J. Membrane Sci.*, 2014, **453**, 292

[23] H. G. Xu, H. Dai and G. N. Chen, *Talanta*, 2010, **81**, 334

[24] S. Ramasundaram, J. H. Jung, E. Chung, S. K. Maeng,S. H. Lee, K. G. Song and S. W. Hong, *Carbon*, 2014, **70**, 179

[25] J. Dai, X. H. Liu, J. H. Yang, N. Zhang, T. Huang, Y. Wang and Z. W. Zhou, *Compos. Sci. Technol.*, 2014, **99**, 59

[26] S. F. Ran and M. Xu, *Chinese J. Polym. Sci.*, 2004, **22**, 123

[27] J. P. G. Villaluenga, M. Khayet, M. A. López-Manchado, J. L. Valentin, B. Seoane and J. I. Mengual, *Euro. Polym. J.*, 2007, **43**, 1132

[28] S. H. Tabatabaei, P. J. Carreau and A. Ajji, *J. Membrane Sci.*, 2008, **325**, 772

[29] X. M. Zhang and A. Ajji, *Polymer*, 2005, **46**, 3385

[30] Y. D. Lv, Y. J. Huang, M. Q. Kong and G. X. Li, *Polym. Test.* 2013, **32**, 179

[31] B. Gu, Q. G. Du and Y. L. Yang, *J. Membrane Sci.*, 2000, 164, 59

[32] C. Chandavasu, M. Xanthos, K. K. Sirkar and C. G. Gogos, *Polymer*, 2002, **43**, 781

[33] G. Chen, Y. K. Lin and X. L. Wang, *J. Appl. Polym. Sci.*, 2007, **105**, 2000

[34] Y. K. Lin, G. Chen, J. Yang and X. L. Wang, *Desalination*, 2009, **236**, 8

[35] H. O. Matsuyama, H. Okafuji, T. Maki, M. Teramoto and N. Tsujioka, *J. Appl. Polym. Sci.*, 2002, **84**, 1701

[36] S. S. Kim and D. R. Lloyd, *J. Membrane Sci.*, 1991, **64**, 13

[37] W. Zhao, Y. L. Su, C. Li, Q. Shi, X. Ning and Z. Y. Jiang, *J. Membrane Sci.,* 2008, **318**, 405

[38] M. M. Meier, L. A. Kanis and V. Soldi, *Int. J. Pharmaceut.*, 2004, **278**, 99

[39] C. L. Bashford, G.M. Alder, J.M. Graham, G. Menestrina and C.A. Pasternak, *J. Membrane Biol.* 1988, **103**, 79

[40] J. W. Chen, J. Dai, J. H. Yang, N. Zhang, T. Huang, Y. Wang and C. L. Zhang, *Ind.Eng.Chem.Res.*, 2014, **53**, 4679

[41] S. Hummers and R. E. Offeman. *J. Am. Chem. Soc.*, 1958, **80**, 1339

[42] J. H. Yang, C. X. Feng, J. Dai, N. Zhang, T. Huang and Y. Wang, *Polym. Int.*, 2013, **62**, 1085

[43] J. Li, W. Cheung and D. Jia. *Polymer* 1999, **40**, 1219

[44] S. J. Liu, C. X. Zhou and W. Yu, *J. Membrane Sci.*, 2011, **379**, 268

[45] J. R. Potts, D. R. Dreyer, C. W. Bielawski and R. S. Ruoff, *Polymer*, 2011, **52**, 5

[46] C. Vallés, I. A. Kinloch, R. J. Young, N. R. Wilson and J. P. Rourke. *Compos. Sci. Technol.* 2013, **88**, 158

[47] J. Z. Xu, Y. Y. Liang, H. D. Huang, G. J. Zhong, J. Lei, C. Chen and Z. M. Li. *J. Polym. Res.*

2012, **19**, 9975

[48] R. Y. Bao, Z. T. Ding, Z. Y. Liu, W. Yang, B. H. Xie and M. B. Yang, *Polymer*, 2013, **54**, 2059

[49] T. Wu, M. Xiang, Y. Cao, J. Kang and F. Yang, *RSC Adv.* 2014, **4**, 36689

[50] T. Wu, M. Xiang, Y. Cao, J. Kang and F. Yang, *RSC Adv.* 2014, **4**, 43012

[51] B.T. Kim, K. Song, and S.S. Kim, *Macromol. Res.*, 2002, **10**, 127

[52] S. C. Yu, Y. P. Zheng, Q. Zhou, S. Shuai, Z. H. Lv and C. J. Gao, *Desalination*, 2012, **298**, 49

[53] Y. Huang and A. J. Kinloch, *Polymer*, 1992, **33**, 1330

[54] R. Bagheri and R. A. Pearson, *Polymer*, 1996, **37**, 4529

[55] X. X. Li, H. Y. Wu, T. Huang, Y. Y. Shi, Y. Wang and F. M. Xiang, *Colloid. Polym. Sci.*, 2010, **288**, 1539

[56] F. Zuo, J. K. Keum, X. M. Chen, B. S. Hsiao, H. Y. Chen, S. Y. Lai, R. Wevers and J. Li, *Polymer*, 2007, **48**, 6867

[57] F. Chu, T. Yamaoka, H. Ide and Y. Kimura, *Polymer*, 1994, **35**, 3442

[58] J. Kotek, M. Raab, J. Baldrian and W. Grellmann, *J. Appl. Polym. Sci.*, 2002, **85**, 1174

Figure captions:

Figure 1: TOM images showing the dispersion of GO in PP/GO and PP/GO/OP-10 samples.

Figure 2: TEM images showing the dispersion of GO and morphologies of initial pores in the PP/GO/OP-10 composite.

Figure 3: (a) Storage modulus and (b) mechanical loss factor of different samples as indicated in the graphs.

Figure 4: DSC heating (a) and cooling (b) curves of different samples as indicated in the graphs.

Figure 5: WAXD profiles showing the crystalline structure of different samples as indicated in the graph.

Figure 6: SEM images showing the pore morphology of different samples as shown in the images. The mean pore size is shown in the image. Samples were obtained at the tensile speed of 50 mm/min, tensile strain of 100% and the ambient temperature of 100 °C.

Figure 7: SEM images showing the pore morphology evolution in the PP/GO/OP-10 composite membrane with the increase of tensile strain. Samples were obtained at the tensile speed of 50 mm/min. (a) 0 wt%, (b) 50%, (c) 100% and (d) 200%

Figure 8: Variation of porosity versus tensile strain of different stretched membranes. The membrane was prepared at tensile speed of 50 mm/min.

Figure 9: SEM images showing the formation of new pores in the adjacent PP matrix around the initial pores.

Figure 10: DSC heating curves showing the melting behavior of stretched membrane. The membrane was prepared at tensile speed of 50 mm/min and tensile strain of 100%.

Figure 11: (a) Comparison of WAXD profiles of the stretched PP/GO/OP-10 membrane obtained at different tensile strain as indicated in the graph, and (b) Variation of crystal size of (110) α crystal face versus tensile strain

Figure 12: Schematic representations showing the pore formation mechanism in the stretched PP/OP-10 membrane (a) and stretched PP/GO/OP-10 membrane (b).
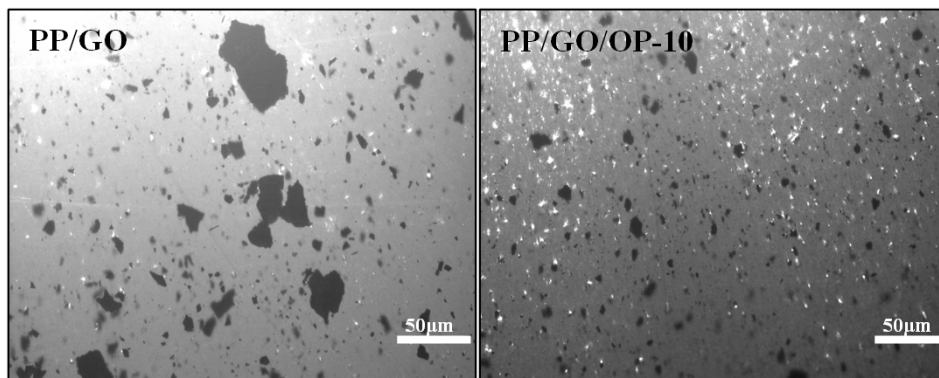
Figure 1
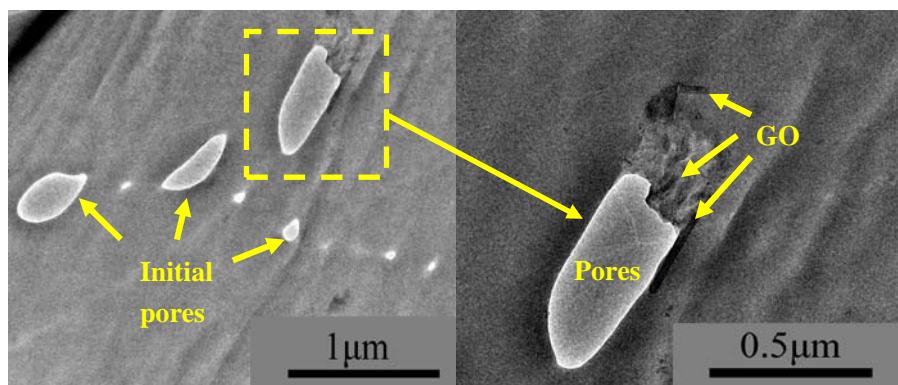
Figure 2
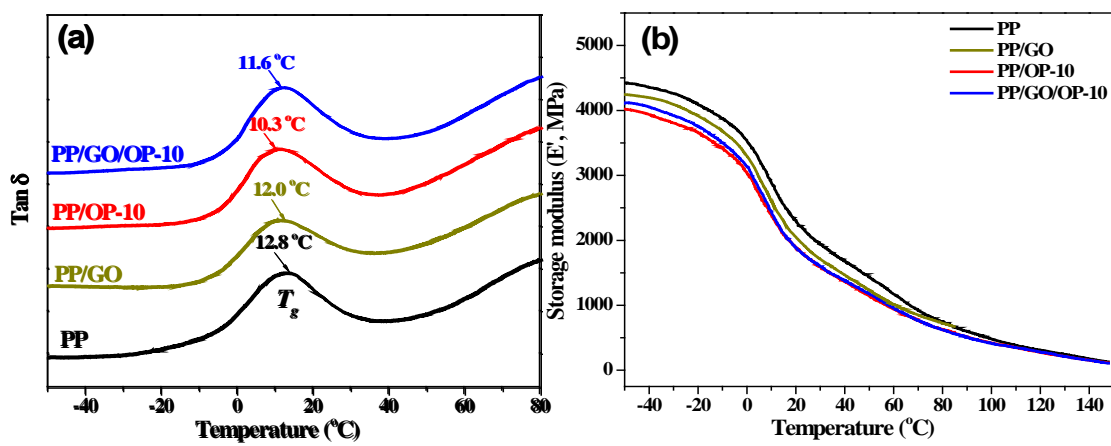
Figure 3
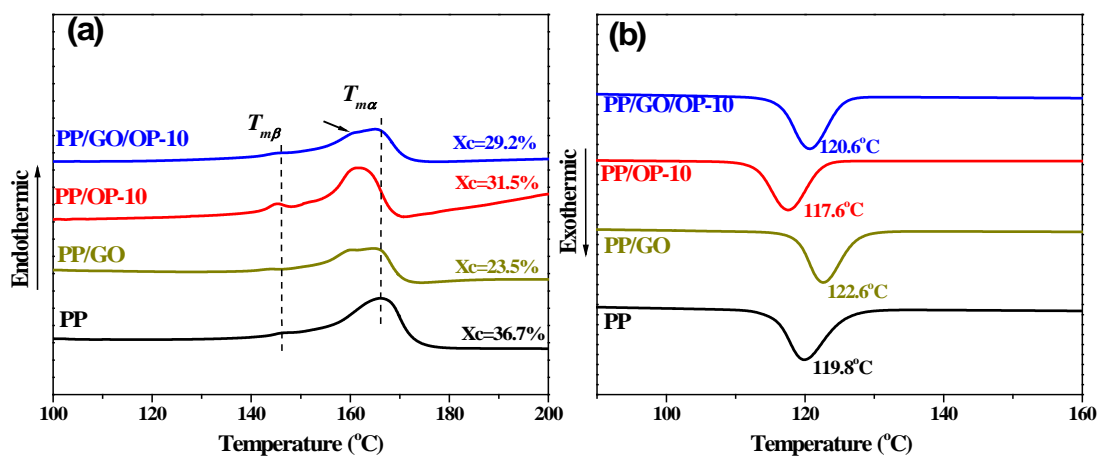
Figure 4
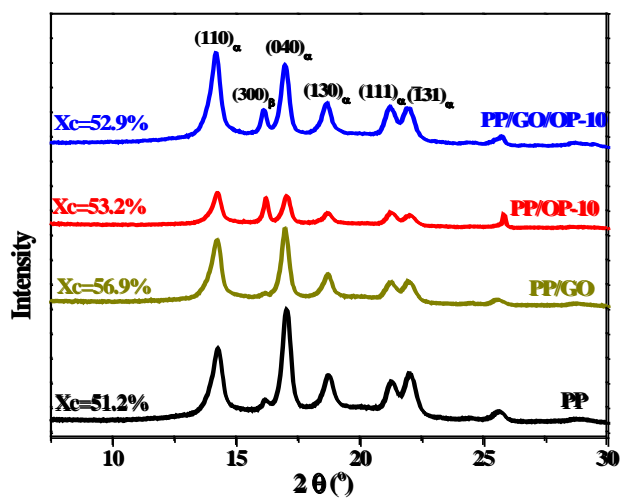
Figure 5
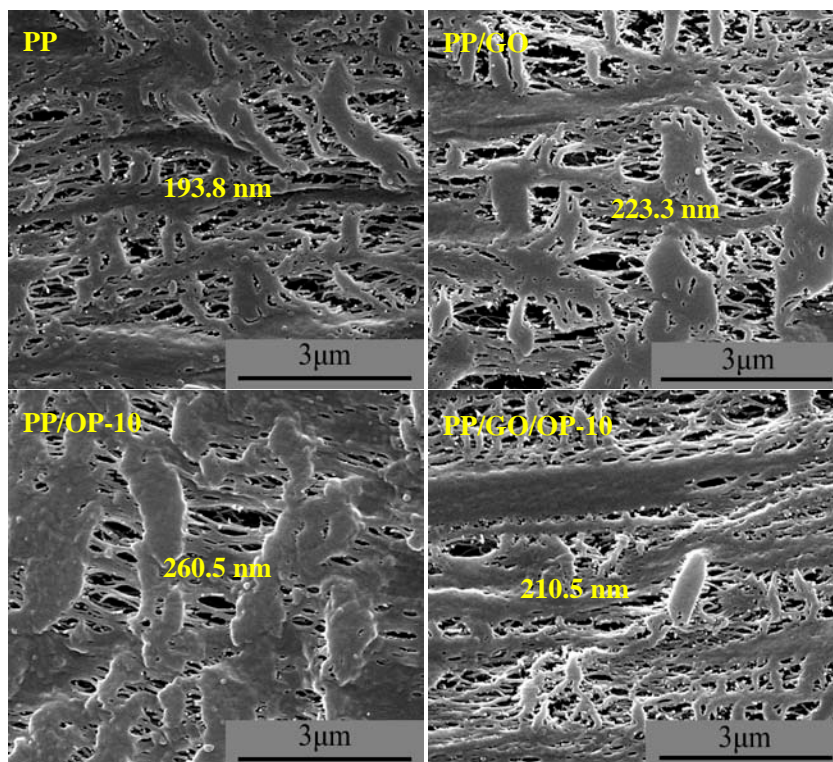
Figure 6
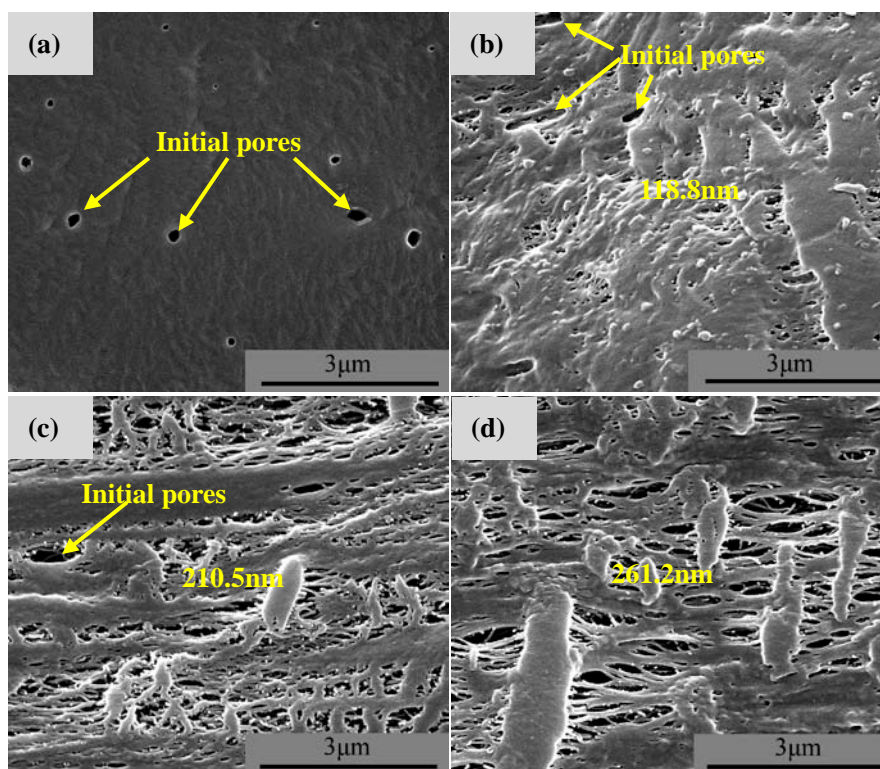
Figure 7
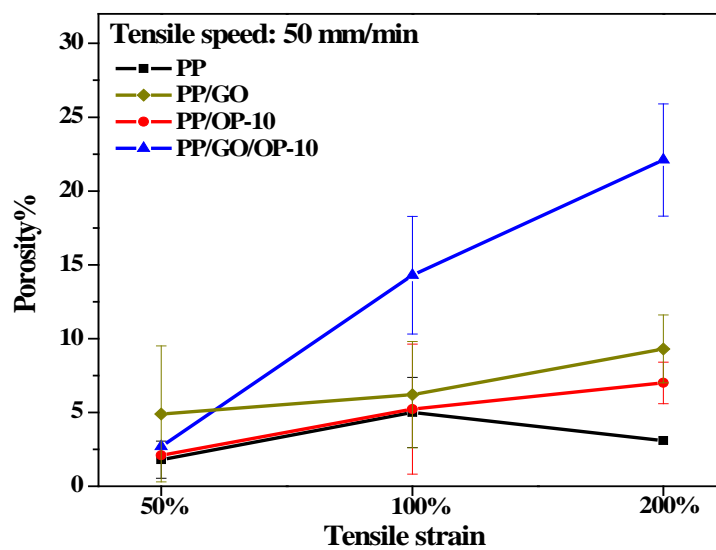
Figure 8
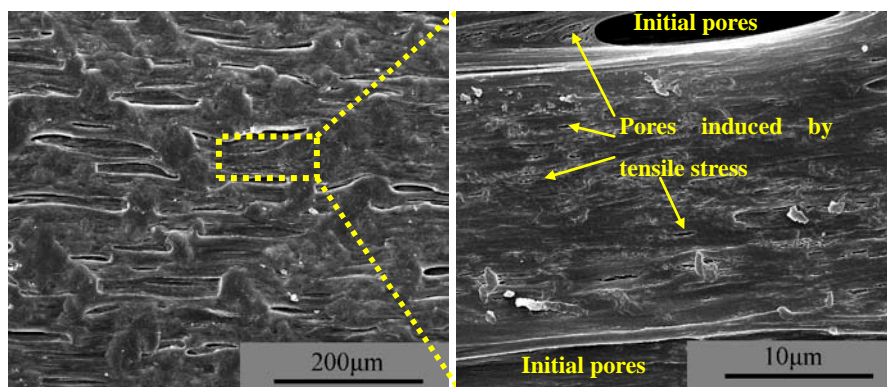
Figure 9

Figure 10

Figure 11

(a)

Initial pores

Spherulite

Lamella
Amorphous

F

Stress inducing pore formation

PP/OP-10 membrane

(b)

GO

Initial pores

Spherulite

Lamella
Amorphous

F

Stress inducing pore formation

Hindrance effect of GO

PP/GO/OP-10 membrane
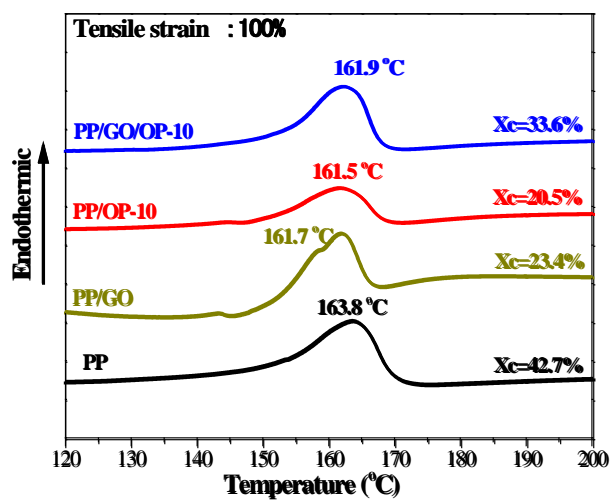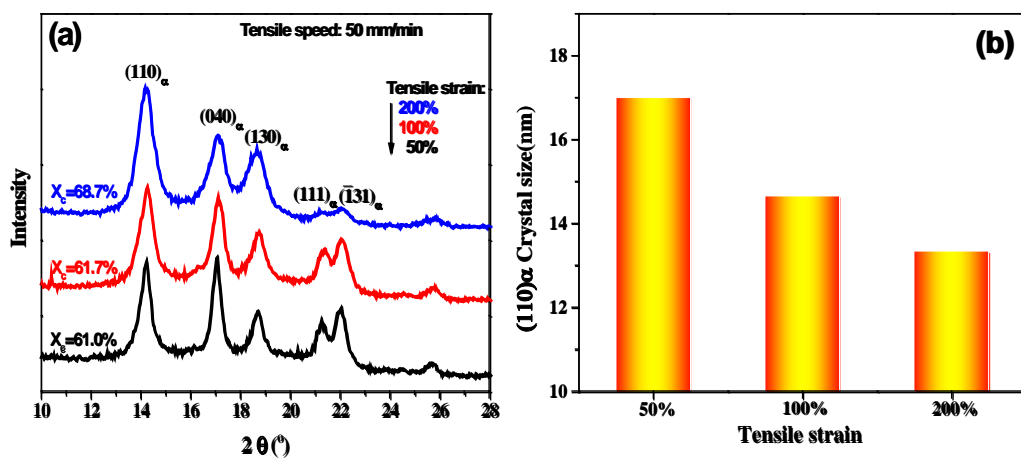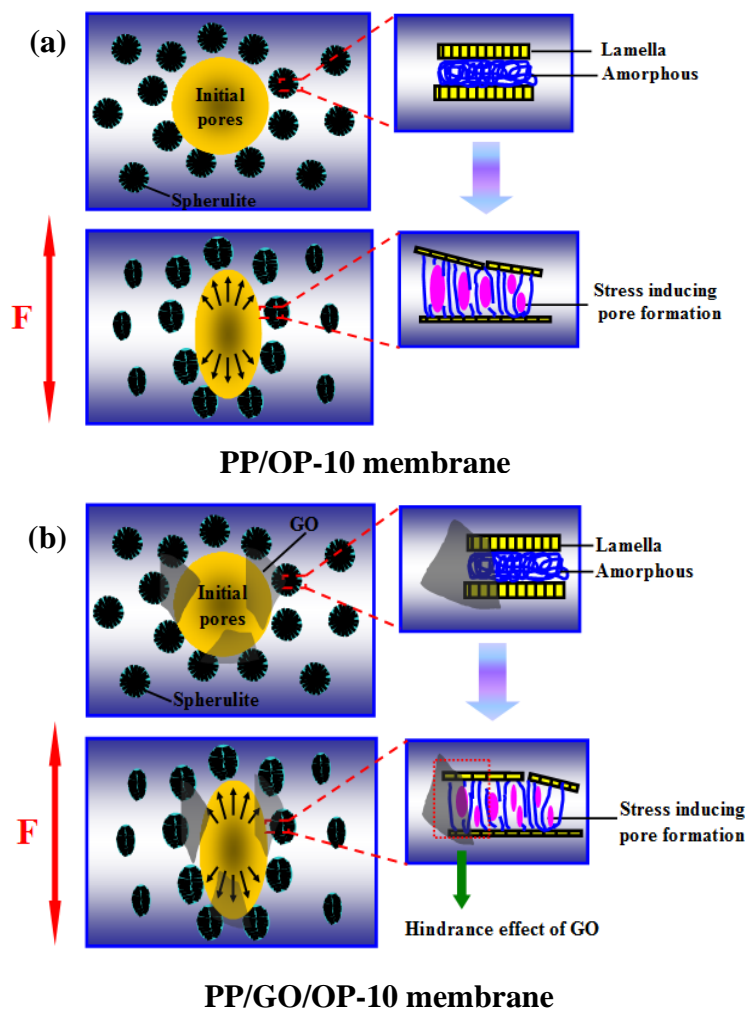
Figure 12

Table of Content use only

Largely enhanced porosity of stretched polypropylene/graphene oxide composite membrane achieved by adding pore-forming agent

Jian Dai, Xian-ling Xu, Jing-hui Yang, Nan Zhang, Ting Huang, Yong Wang,

Zuo-wan Zhou, Chao-liang Zhang
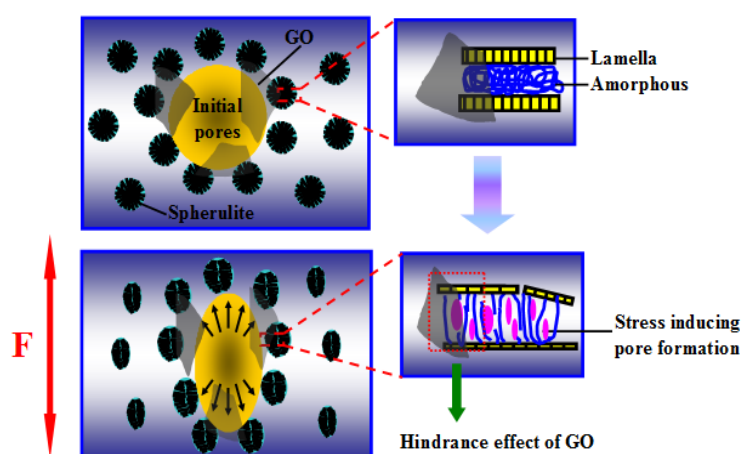
With the combined effects of pore-forming agent and graphene oxide, largely enhanced porosity is achieved for the stretched PP composite membrane.